

# Coupled Electro-Thermal Modeling of Magnetic Bearing Systems

Shuqin Liu

Dept. of Electrical Engineering  
Shandong University  
Jinan, 250061, China  
lshuqin@sdu.edu.cn

Chris Mi

Dept. of Electrical and Computer Engineering  
University of Michigan-Dearborn  
Dearborn, MI, 48128, USA  
chrismi@umich.edu

**Abstract** –This paper presents coupled electromagnetic and thermal modelling of active magnetic bearing systems. In magnetic bearing systems, the electric, magnetic, eddy current and thermal processes are intrinsically coupled. There are two major sources of heat generated in magnetic bearing: the heat generated by the DC current in the excitation coils and the heat generated by the eddy current in the high speed rotating parts. The eddy current is not uniformly distributed in the rotor and thrust bearing. In this paper, the magnetic field is first modelled using 2D/3D finite element analysis (FEA). The eddy current information obtained in FEA is then transferred to thermal FEA model to perform thermal analysis. Hot spots can be identified in this procedure.

By using Ansoft's Electromagnetic package, the 2D/3D FEA is coupled with thermal FEA through e-Physics. Data can be automatically linked and exchanged between the magnetic and thermal models.

The experiment data on a test platform validated the proposed model.

**Index Terms** – Magnetic bearing, Electrical field, Thermal field, Coupled model.

## I. INTRODUCTION

Magnetic bearing systems are generally operated at high speeds; therefore heat concentration may occur in the rotor and thrust bearing. High temperature may affect the safe operation of the bearing system such as change in magnetic force, magnetic stiffness, and result of instability. It is critical to accurately predict the temperature gradients in a magnetic bearing system. Accurate temperature calculation also helps the selection of bearing architecture, material, and the design of cooling system [1-4].

There are two major sources of heat generated in magnetic bearing: the heat generated by the DC current in the excitation coils and the heat generated by the eddy current in the high speed rotating parts. The former is called copper loss, and the latter is called iron loss. They depend on the temperature and are non-linear effects. The iron loss is mainly eddy current especial for rotor and thrust bearing, because they are made of solid iron not lamination.

The eddy current is not uniformly distributed in the rotor and thrust bearing and is relative to frequency. Research on thermal network of magnetic bearing and high temperature active magnetic bearing has been carried out [1] - [2]. The purpose of this paper is to present the results from 2D/3D finite element analysis (FEA) calculations concerning the magnetic field and eddy currents induced in conducting rotor and thrust bearing. Furthermore, the coupled analysis allows the calculation of the temperature gradients of the magnetic bearings.

## II. STATIC MAGNETIC FIELD

### A. Modeling the Cylindrical Thrust Bearing

The magnetostatic field is first analysed using 2D/3D finite element analysis (FEA). The magnetic force of the thrust bearing can be calculated based on the 2D FEA. The thrust bearing consists of thrust plate, two coils and two iron poles. The construction of the thrust bearing is shown as Fig. 1. Since the thrust bearing is axisymmetric, we can use the cylindrical coordinate system  $(r, \phi, z)$  in performing the 2D FEA. The cylindrical symmetrical model is as follow:

$$\frac{\partial}{\partial \phi}(E, B, A) = 0 \quad (1)$$

where  $E$  is electric field intensity;  $B$  is magnetic flux density;  $A$  is vector magnetic potential.

The vector field satisfies the following equation:

$$\frac{\partial}{\partial z} \left( v \frac{\partial A}{\partial z} \right) + \frac{\partial}{\partial r} \left( v \frac{\partial A}{\partial r} \right) + J_s = r \frac{\partial A}{\partial i} \quad (2)$$

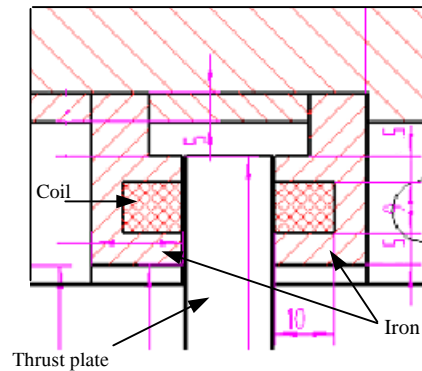


Fig. 1 The structure of thrust magnetic bearing.

\* This work is partially supported by Development plan of Science and Technology of Shandong Province, Grant #031110120 and Jinan City Grant #031061.

where  $J_s$  is the applied current density that is uniform throughout the cross section of the conductor. The parameters of the thrust bearing are shown in Table I.

TABLE I  
PARAMETERS FOR THRUST BEARING

Name	Value	Units
Rotor diameter	40	mm
Thrust plate diameter	80	mm
Gap	0.5	mm
Coil window width	6	mm
Inside ring diameter	50	mm
Outside ring diameter	80	mm
Coil window high	8	mm
Actuator current density	3.5	A/mm <sup>2</sup>

### B. The Magnetic Field of Thrust Bearing

The 2D/3D FEA was performed assuming linear, isotropic materials and neglecting hysteresis, saturation, leakage and fringing flux. Fig. 2 show the magnetic flux density obtained using 2D FEA and Fig. 3 shows the flux distribution at 0Hz.

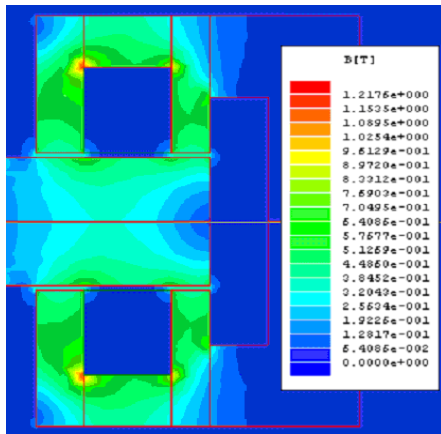


Fig. 2 The Magnetic flux density of the thrust bearing(2D)

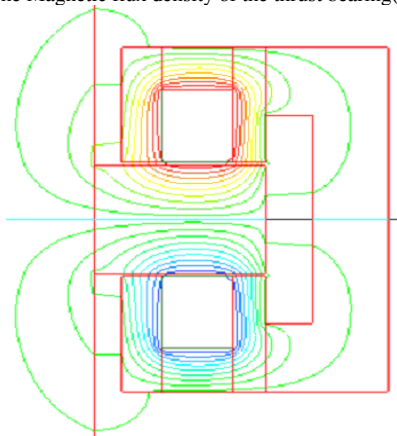


Fig. 3 The Magnetic field of the thrust bearing

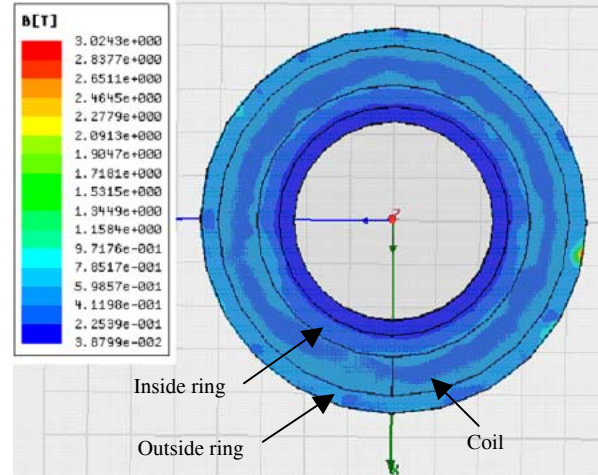


Fig. 4 The Magnetic flux density of the thrust bearing(4D)

Fig. 4 is shows the magnetic flux density obtained using 3D FEA. The 3D FEA can reflect the leakage flux and fringing effects in the gap. It can be observed from Fig. 4 that the average value of flux density is 0.5T which confirms to our designed. The electromagnetic force including inside ring and outside ring can then be calculated.

Fig. 3 shows that the flux distributes mainly in the surface layer of the iron. When flux leaves or enters the iron, flux lines are vertical to the surface of the air gap. Based on the directions of the flux lines and taking into account the non-uniformity of flux density in the air gap, we calculate the electromagnetic force which attracts the thrust plate, the outside ring and inside ring. The results are show in Table II.

TABLE II  
THE FORCE OF THRUST BEARING(OUTSIDE RING)

Name	Value	Units
Inner ring $F(x)$	1.81	N
Inner ring $F(y)$	-8.99	N
Inner ring $F(z)$	-137.81	N
Outer ring $F(x)$	3.96	N
Outer ring $F(y)$	-2.25	N
Outer ring $F(z)$	137.84	N

The force  $F(z)$  is the suspend force that is needed to support the rotor at the correct position. The forces  $F(x)$  and  $F(y)$  are generated by leakage and fringing effect.

### III. EDDY CURRENT FIELD

Because radial magnetic bearing can be made of very thin and perfectly insulating sheets between touching, eddy current can be reduced. However, the thrust bearing plates are made of solid steel which will cause eddy currents. The eddy field is analyzed using 3D. For high rotating speed the magnetic fields frequency is very high. The time-varying (AC) magnetic fields at a given frequency can be analysed using 3D FEA as shown in (3). The eddy current density ( $J$ ) can be calculated using equation (4).

$$\nabla \times \frac{1}{\sigma + j\omega\epsilon} \nabla \times H = j\omega\mu H \quad (3)$$

$$J = \nabla \times H = (\sigma + j\omega\epsilon)E \quad (4)$$

where  $\omega$  is angular frequency in radian,  $H$  is magnetic field intensity,  $\mu$  is permeability,  $\sigma$  is electrical conductivity,  $\epsilon$  is permittivity.

The current density ( $J$ ) and magnetic flux density ( $B$ ) are calculated from the magnetic field intensity ( $H$ ). We only consider the sinusoidal eddy current field. Fig. 5 shows the eddy current field vector in the thrust plate at 200Hz. Fig. 6 shows the eddy current density in the thrust plate at 200Hz. The eddy current value is about 0.77 T—1.50 T. The average eddy current density is about 0.7A/mm<sup>2</sup>. This value indicates that the eddy current effect is small at 200 Hz. Therefore, at low frequency, the eddy loss can be neglected.

Fig. 7 shows the eddy current field vector at 400Hz. The magnetic flux density  $B$  is about 0.72T—2.12T. The average eddy current density is approximately 1.0A/mm<sup>2</sup>.

We also calculate the eddy current field of the thrust plate at 600Hz, 800Hz and 1000Hz. The results indicate that the flux density  $B$  induced by eddy current field become larger when the frequency increases and the eddy density value also increase with frequency.

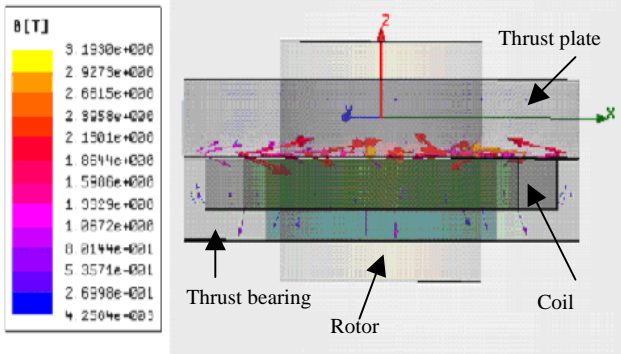


Fig. 5 The eddy current field vector(200Hz)

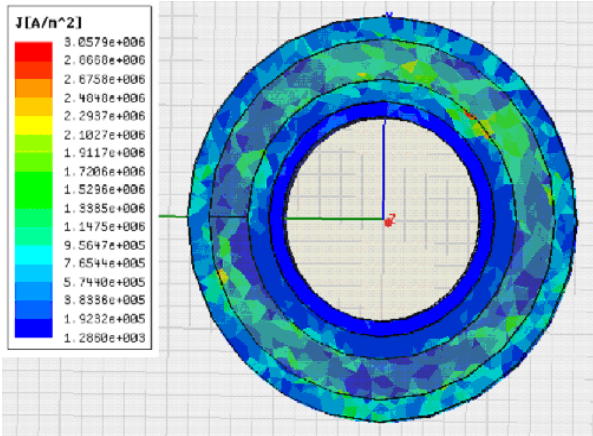


Fig. 6 The eddy current density(200Hz)

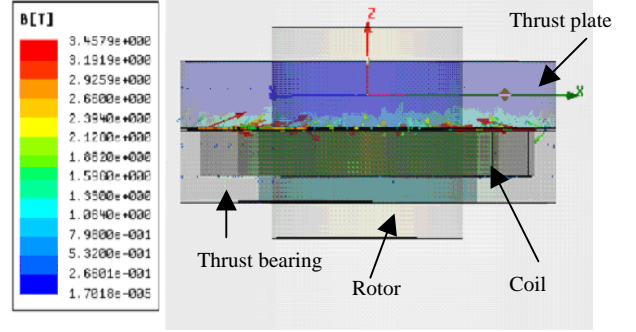


Fig. 7 The eddy current field vector(400Hz)

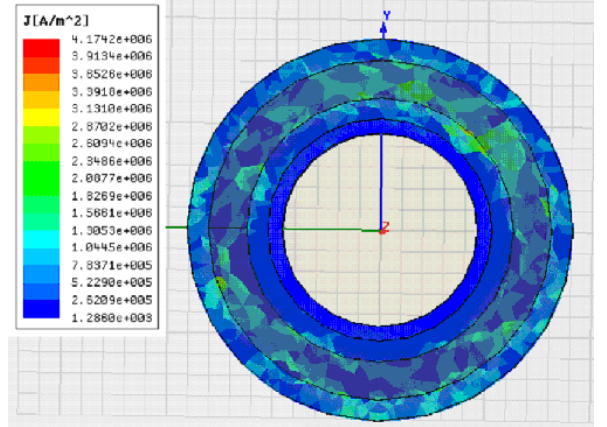


Fig. 8 The eddy current density(400Hz)

The eddy current of the thrust plate at 1000Hz is shown in Fig. 9. The magnetic flux density  $B$  is about 2.0 T.

We also calculate the applied current density in the thrust bearing in order to calculate the copper loss.

#### IV. ELECTRO-THERMAL FIELD ANALYSIS

##### A. The temperature field analysis

We calculate the static thermal fields of the magnetic bearing. The static thermal field calculation includes computing steady state temperatures. The source of the heat are from the copper loss and eddy current loss. The quantity solved is the temperature ( $T$ ). The thermal field is analysed by incorporating the electromagnetic field solutions from 2D/3D electromagnetic FEA.

The temperature field is computed by using a cylindrical coordinate system ( $r, \phi, z$ ) according to the Fourier thermal equation shown in (5).

$$\frac{1}{r} \frac{\partial}{\partial r} \left( \lambda r \frac{\partial T}{\partial r} \right) + \frac{1}{r} \frac{\partial}{\partial \phi} \left( \lambda \frac{\partial T}{\partial \phi} \right) + \frac{\partial}{\partial z} \left( \lambda \frac{\partial T}{\partial z} \right) + p_v = \frac{\partial}{\partial r} (vcT) \quad (5)$$

where:  $\lambda$  is the material thermal conductivity [W/(m·k)];  $T$  is temperature [K];  $p_v$  heat inner source [W/m<sup>3</sup>];  $\nu$  mass density [kg/m<sup>3</sup>];  $c$  material heat race [J/kg·K].

In this paper the simplified equation with cylindrical coordinate system ( $r, \phi, z$ ) is used.

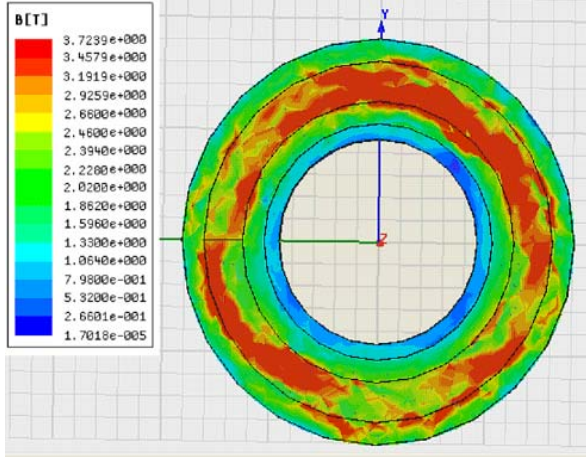


Fig. 9 The eddy current density(1000Hz)

$$\frac{1}{r} \frac{\partial}{\partial r} \left( \lambda r \frac{\partial T}{\partial r} \right) + \frac{\partial}{\partial z} \left( \lambda \frac{\partial T}{\partial z} \right) + p_v = \frac{\partial}{\partial r} (vcT) \quad (6)$$

The thermal field is coupled with eddy current field, so the eddy loss and iron loss are also computed. The equation shown in (7) include two parts:

$$Q = \frac{1}{2\sigma} J \cdot J^* + \frac{1}{2} \omega \mu^{rr} H \cdot H^* \quad (7)$$

where  $J$  is current density,  $\sigma$  is electrical conductivity,  $\omega$  is eddy field angular frequency in radian,  $\mu$  is magnetic conductivity,  $H$  is magnetic field intensity. The superscript represents complex number.

The average value of temperature is calculated by equation (8).

$$T_{avg} = \frac{1}{vol(Object)} \iiint_{Object} T dv \quad (8)$$

After the temperature field is calculated hotspot and the cold spot called can be identified for the thrust bearing.

### B. The Thermal Sources and Thermal Boundary Conditions

The heat sources include eddy current and the ohmic loss of DC current in the excitation coils. The eddy current coupled directly to the thermal field. The  $J$  vector in the thrust bearing is first calculated; then the temperature distribution due to induced eddy currents is calculated. The eddy current loss is directly mapped to the thermal field.

Setting up thermal boundary conditions is very important for calculating temperature field. There are three heat boundary conditions, conduction, convective and radiation.

Equation (9) is the conduction boundary condition.

$$-k \nabla T \cdot n = -[k] \frac{\partial T}{\partial n} = h(T, r, \phi, z)(T - T_a) \quad (9)$$

where  $T$  is the surface temperature,  $T_a$  is the ambient temperature,  $h$  is the heat transfer coefficient.

Equation (10) is the convective and radiation boundary condition.

$$-k \nabla T \cdot n = c|T - T_a|^{FEXP} (T - T_a) + F \cdot B(T^4 - T_r^4) \quad (10)$$

where  $T_a$  is the ambient temperature of the cooling fluid,  $c$  is the convective exchange heat coefficient.  $FEXP$  is convective exponential, its value is between 0 and 1.  $T_r$  is radiation reference temperature,  $B$  is constant, the value is equal to  $5.67 \times 10^{-8} \text{W}/(\text{m}^2\text{K}^4)$ ;  $F$  is the radiation emissivity, the value is between 0 and 1.

### C. The Results

It is rather difficult to determine the heat transfer coefficient of the insulation layer. Because it is very thin, its boundary condition is also difficult to determine. It is also difficult to determine the convective coefficient and radiation emissivity in the air gap. Because fluid flow is not modelled – there is no convective or radiation heat exchange between thrust bearing and thrust plate. It is difficult to calculate the air velocity distribution for radiation boundary condition and convective boundary condition (heat transfer) because the air gap is very small (0.5mm). In fact the boundary conditions are determined by calculating different conditions and calibrate by experiment results. Figure 10 is the temperature of thrust plate with eddy current. The influence of eddy current on temperature is transferred by e-Physics. The ambient temperature is set  $25^\circ\text{C}$ . The solve region is 5 times as large as the object. Figure 10 shows that where the eddy current is big, the temperature is high.

### V. CONCLUSION

This paper has discussed a preliminary study on coupled electromagnetic-thermal analysis of active magnetic bearing. Due to the geometric complexity of the radial and thrust bearing, 3D FEA is usually necessary in getting accurate thermal gradients. Eddy current plays an very important role in the temperature rise of the thrust plates at high frequencies. Detailed thermal coefficients are critical to achieve accurate thermal field. Further studies are being carried out to validate the accuracy of the proposed method.

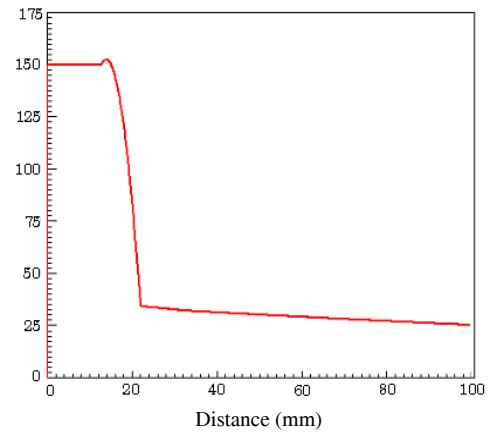


Fig 10 The temperature of thrust plate (with eddy)

## REFERENCES

- [1] Luc Burdet, Beat Aeschlimann, Roland Siegwart, "Thermal model for a high temperature active magnetic bearing," Ninth International Symposium on Magnetic Bearings, Lexington, Kentucky, USA, August, 2004
- [2] Xu L., Wang L., Schweitzer G. "Development of magnetic bearings for high temperature suspension," ISMB-7, Zurich 2000
- [3] Torbjorn A. Lembke, "3D-FEM Analysis of a low loss homopolar induction bearing," Ninth International Symposium on Magnetic Bearings, Lexington, Kentucky, USA, August, 2004
- [4] Siegwart R, Bleuler H, and Traxler A, Industrial Magnetic Bearings – Basics and Application, Gordon and Breach Science Publisher, Amsterdam, 2000
- [5] Guoqiang Liu, Lingzhi Zhao and Jiya Jiang, Ansoft Finite Element Analysis for Engineering Electromagnetic Field, Beijing, 2005